Supplementary Information

Thermodynamic and Structural Insights into Nanocomposites Engineering by Comparing Two Materials Assembly Techniques for Graphene

Jian Zhu,[1] Huanan Zhang,[1] Nicholas A. Kotov[1,2,3,4*]

[1]Department of Chemical Engineering, [2]Department of Materials Science and Engineering, [3]Department of Biomedical Engineering, [4]BioInterface Institute, University of Michigan, Ann Arbor, 48109, USA

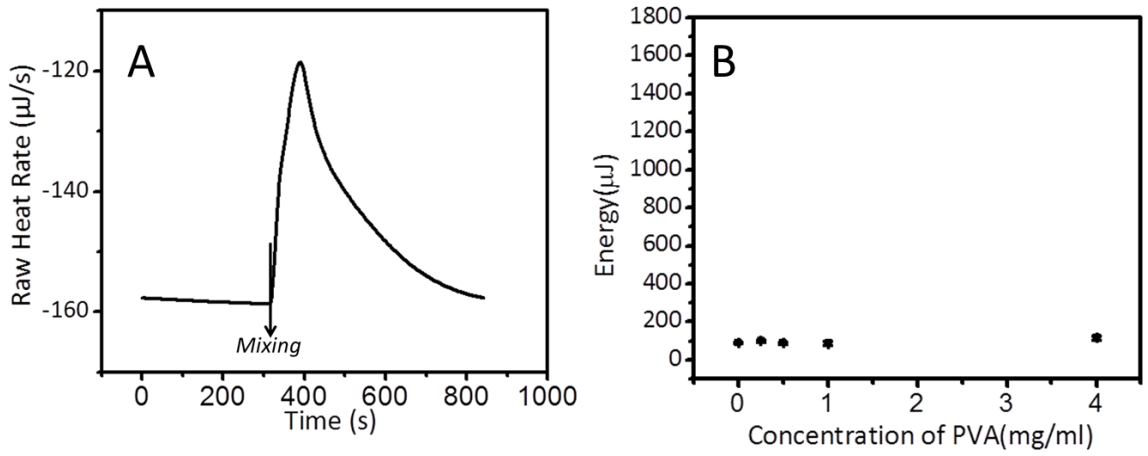

Figure S1. (a) Typical raw heat rate vs. time when mixing PVA and RG solutions. (b) Mixing enthalpies for PVA and DI water for different concentrations of PVA. The scale of the "Energy" axis is identical to that in Figure 1b.

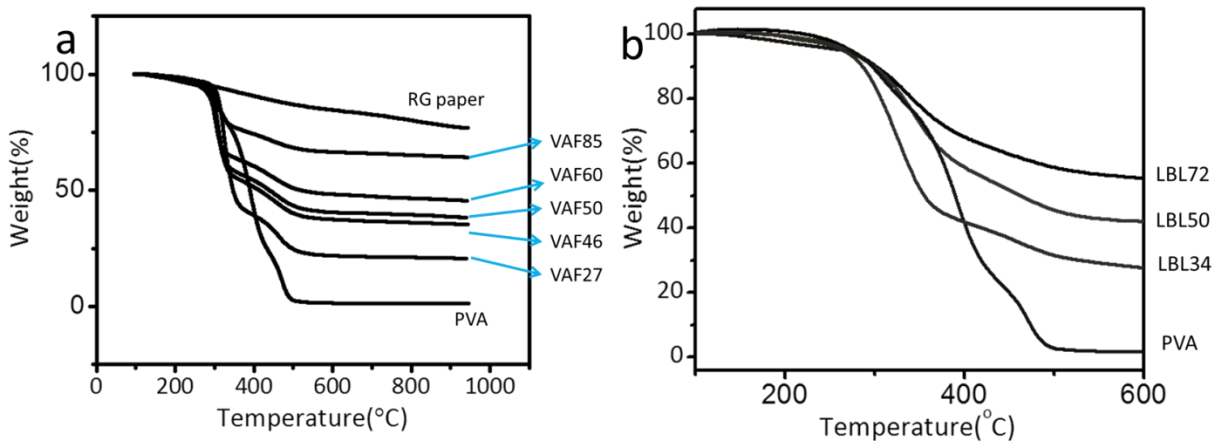

Figure S2. TGA curves for (a) VAF and (b) LBL composites from PVA and RG, pure PVA and RG paper. RG fractions are calculated from the residual weights at 600 ℃.

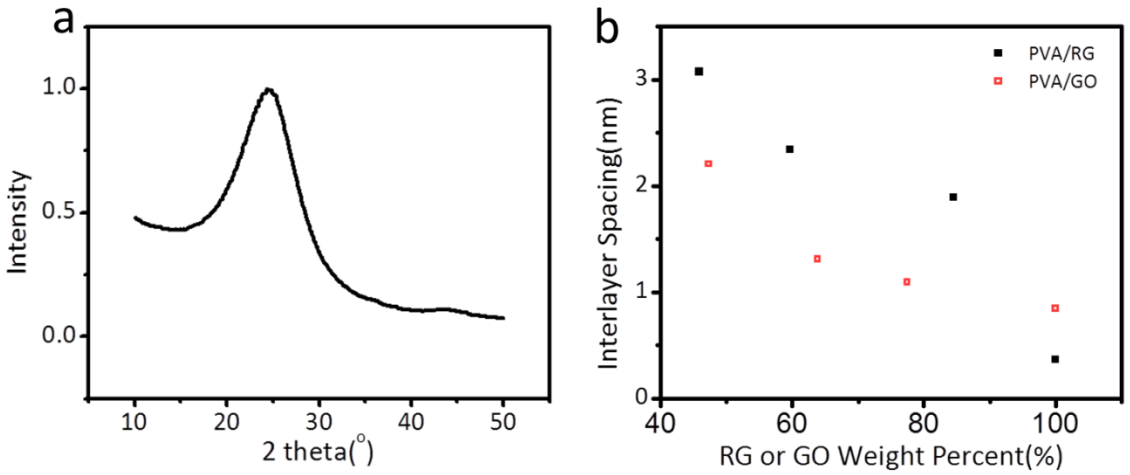

Figure S3. (a) XRD scattering of VAF-made RG paper without any polymer. (b) Comparison of interlayer spacing of PVA/RG and PVA/GO composites made by VAF at different RG weight fractions. The data for PVA/GO composites are taken from Ref.[1]

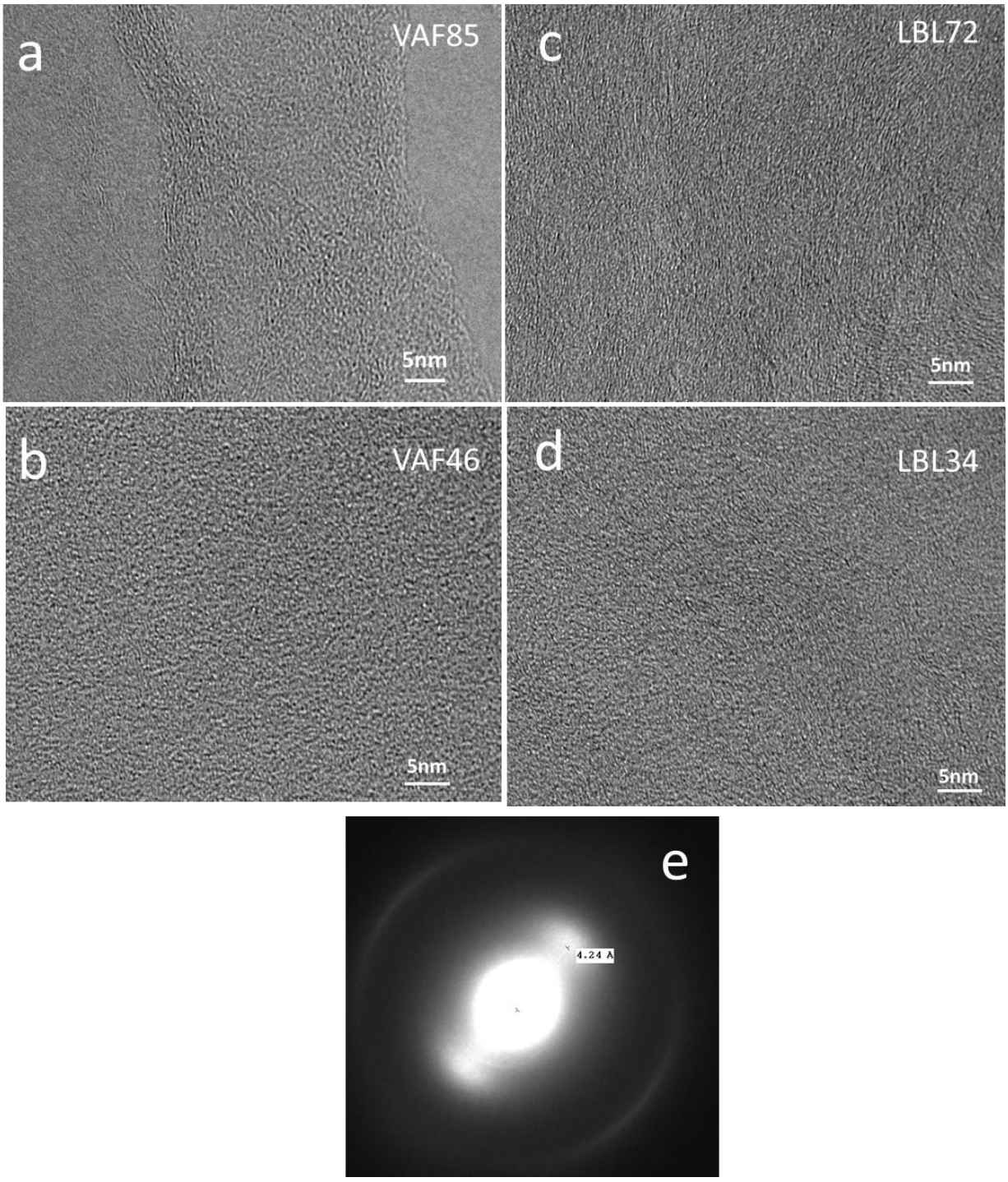

Figure S4. High resolution TEM images of (a) VAF85, (b) VAF46, (c) LBL72, and (d) LBL34 cross-sections. (e) The selected area electron diffraction of LBL34.

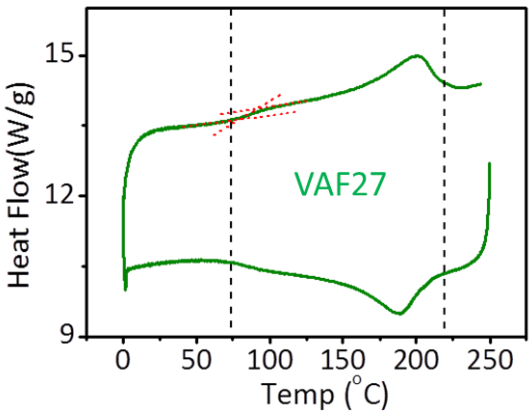

Figure S5. DSC curve for VAF27 showing the glass transition.

Theoretical Predictions of Mechanical Properties of Layered PVA/RG Composites.

A. Known Parameters used in Calculations:

For calculations of Young's moduli of composites:

Young's Modulus of RG:[2,3] E_f=250GPa

Poisson ratio of RG: v_f=0.41

Aspect ratio of *RG* sheets: $\alpha = \frac{L}{d} = 100 \sim 1000$, where *L* and *d* are the average diameter and thickness of the sheet respectively. (Figure S6e)

Young's Modulus of PVA: E_m=3.52GPa

Poisson ratio of PVA: ν_m=0.45

Shear Modulus of PVA: $G_m=E_m/[2\times(1+\nu_m)]=1.21GPa$

For calculations of ultimate tensile strength of composites:

Strength of RG:[4] σ_f = 42GPa

Shear strength of PVA: τ_y = 45 MPa

Critical aspect ratio:[5,6] $\alpha_c = \sigma_f/\tau_y$=1000

Tensile strength of polymer: σ_m = 90 MPa

B. Theoretical Calculations of Young's Modulus:

1. **Voigt Model**[5] (Figure S6c)

$E=V_fE_f+(1-V_f)E_m$ **(Eq.1)**

2. ***Reuss Model***[5] (Figure S6d)

$1/E=V_f/E_f+(1-V_f)/E_m$ **(Eq.2)**

3. ***Padawer&Beecher Model***[5,7] (Figure S6e)

$E=V_fE_f(MRF)+(1-V_f)E_m$, where $MRF=1-\tanh(u)/u$, and $u=\alpha\{G_mV_f/[E_f*(1-V_f)]\}^{0.5}$ **(Eq.3)**

4. ***Riley Model***[5,8] (Figure S6e)

$E=V_fE_f(MRF)+(1-V_f)E_m$, where $MRF=1-\ln(1+u)/u$, and $u=\alpha\{G_mV_f/[E_f*(1-V_f)]\}^{0.5}$ **(Eq.4)**

5. ***Mori-Tanaka Model***[9] (Figure S6f)

   $E=E_{11}=1/S_{11}$, where S11 is the element in compliance tensor S of the composite. **(Eq.5)**

   $S=(V_mS_m+V_fS_fB)(VmI+V_fB)^{-1}$,

   $B=C_fA(C_m)^{-1}$,

   $A=[P_mC_m^{-1}(C_f-C_m)+I]^{-1}$

   C_m, S_m and C_f, S_f are the modulus and compliance tensors of the matrix and the filler respectively. I is identity tensor, A and B are referred to as stress and stress concentration tensor respectively. P_m is the well-known Eshelby's tensor, and depends on the elastic properties of the matrix and the shape of the fillers.

6. ***Halpin-Tsai Model***[10] (Figure S6e)

$$E = E_m\left[\frac{1+\eta\xi V_f}{1-\eta V_f}\right],\ \eta = \frac{\frac{E_f}{E_m}-1}{\frac{E_f}{E_m}+\xi},\ \xi = 2\alpha/3 \qquad \textbf{(Eq.6)}$$

Comment: The Young's modulus (E) of PVA/RG layered composites could be predicted by relating the matrix and filler elements using two different approaches. In the Voigt model, the elements are in parallel with each other and experience the same strain (Figure S6c). The value of Young's modulus E is then given by Eq. 1. The other approach is represented by the Ruess model where all the elements are in series and undergo the same stress (Figure S6d). The value of Young's modulus E is then given by Eq. 2. The Voigt and Reuss models predict the upper and lower bounds of E, respectively.

Figure S6e depicts the model of the layered PVA/RG composites, where discontinuous sheets are parallel to each other in a matrix. The sheets are embedded in the matrix and load is transferred from matrix to the sheet by shear force at the interface. A "shear lag" analysis was developed in Padawer and Beecher model (Eq.3) taking into account the shear modulus of the matrix and aspect ratio of the filler. The Riley model (Eq. 4) considers the interactions between adjacent sheets while the others do not.

Another approach of predicting the E of layered composites is through the Mori-Tanaka model (Eq. 5).[9,10] It takes into account the overlapping stress field of neighboring fillers. This model can effectively predict the reinforcing effects of fibers, spheres and sheets by using either prolate or oblate spheroids (Figure S6f). Remember that when the filler has geometry of sheets, the aspect ratio in this model is defined as $1/\alpha$, where $\alpha = L/d$ (Figure S6e). This model is based on the Eshelby's equivalent inclusion method and the Mori-Tanaka's average stress theory.

The E of this structure (Figure S6e) can also be predicted by a semi-empirical Halpin-Tsai model (Eq. 6). Since the empirical parameter ξ is usually calculated by the Mori-Tanaka model,[9] the curves based on those models usually overlap.

When the aspect ratio α of sheets is high enough (>1000), the predictions for *E* based on models 3–6 are close to that those obtained from the Voigt model or the rule of mixtures (Figure S6g). *To be noted here, all those models presume that matrix is firmly bonded to the RG (i.e. stress transfer at the interface is ideal.*

The values of Young's moduli measured in this study are close to those predicted by the Reuss model (Figure 7) while all the other models greatly overestimate their mechanical properties. Considering the assumptions and the directionality of the hard and soft segments in the Reuss model (Figure S6d), the approximate coincidence is likely to be fortuitous. The strong discrepancy with predictions by other models describing the directionality of the sheets much closer to the actual structure of LBL and VAF composites should be attributed to the non-ideal stress transfer at the RG-PVA interface. The reasons behind non-ideality of the stress transfer even for small deformations can be multiple and need more extensive experimental studies.

C. Theoretical Calculations of Ultimate Strength:

The aspect ratio of RG is typically smaller than critical aspect ratio, so that the RG composites should rupture under the sheets pull-out mode. [5,6]

Thus the strength of composites (σ_{ult}) can be calculated in the structure similar to Figure S6e using the Rule of Mixtures:[5,6]

$$\sigma_{ult}=0.5V_p\tau_i\alpha+(1-V_p)\sigma_m$$

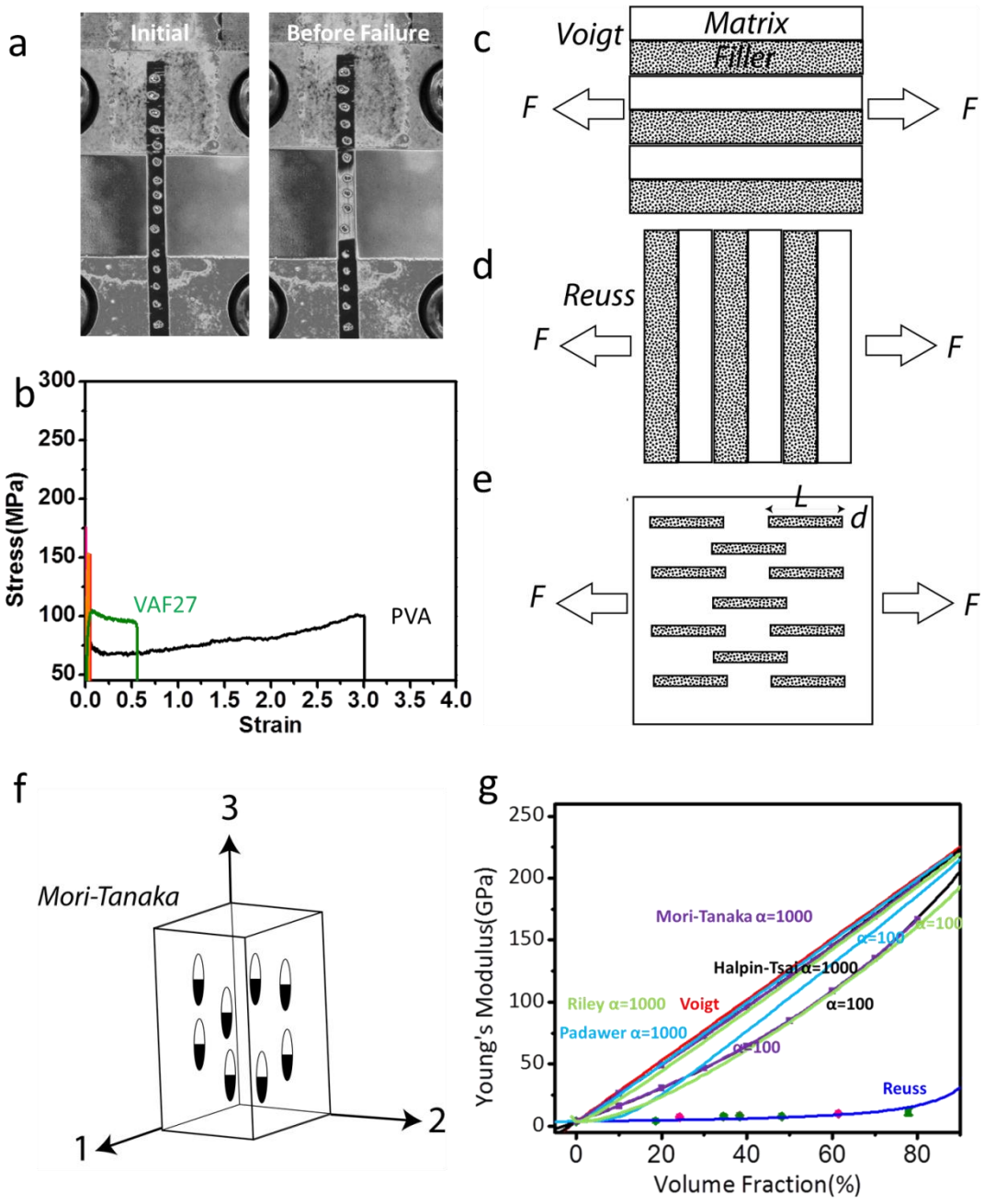

Figure S6. (a) A photograph of LBL50 sample strip with gauge marks stretched between two grips at the initial and before-failure states. (b) Stress-strain curves for VAF27 and PVA. c, d, e, f) Different configurations of layered structures theoretical models are based on. g) Predictions of Young's moduli of LBL/VAF composites with specific volume fractions based on Voigt (red), Reuss (blue), Padawer (light blue), Riley(light green), Mori-Tanaka (Purple) and Halpin-Tsai (black) for different aspect ratios of the filler (α).

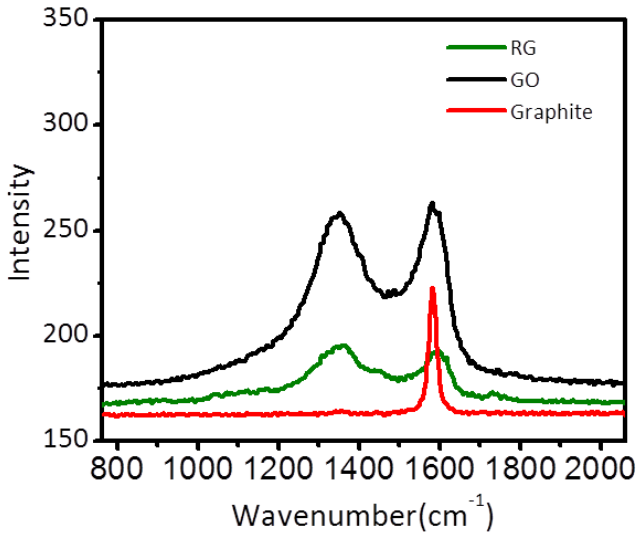

Figure S7. Raman spectra of GO, RG and graphite.

REFERENCES FOR SUPPLEMENTARY INFORMATION

1. Putz, K.W., Compton, O.C., Palmeri, M.J., Nguyen, S.T. & Brinson, L.C. High-Nanofiller-Content Graphene Oxide–Polymer Nanocomposites via Vacuum-Assisted Self-Assembly. *Adv. Funct. Mater.* **20,** 3322-3329 (2010).
2. Gomez-Navarro, C., Burghard, M. & Kern, K. Elastic properties of chemically derived single graphene sheets. *Nano Lett.* **8,** 2045-2049 (2008).
3. Suk, J.W., Piner, R.D., An, J. & Ruoff, R.S. Mechanical Properties of Monolayer Graphene Oxide. *ACS Nano* **4,** 6557-6564 (2010).
4. Paci, J.T., Belytschko, T. & Schatz, G.C. Computational Studies of the Structure, Behavior upon Heating, and Mechanical Properties of Graphite Oxide. *J. Phys. Chem. C* **111,** 18099-18111 (2007).
5. Jackson, A.P., Vincent, J.F.V. & Turner, R.M. The Mechanical Design of Nacre. *Proceedings of the Royal Society of London. Series B. Biological Sciences* **234,** 415-440 (1988).
6. Bonderer, L.J., Studart, A.R. & Gauckler, L.J. Bioinspired Design and Assembly of Platelet Reinforced Polymer Films. *Science* **319,** 1069-1073 (2008).
7. Padawer, G.E. & Beecher, N. On the strength and stiffness of planar reinforced plastic resins. *Polym. Eng. Sci.* **10,** 185-192 (1970).
8. Lusis, J., Woodhams, R.T. & Xanthos, M. The effect of flake aspect ratio on the flexural properties of mica reinforced plastics. *Polym. Eng. Sci.* **13,** 139-145 (1973).
9. van Es, M.A. *Polymer-clay Nanocomposites: The Importance of Particle Dimensions*, (2001).

10. Liang, J., *et al.* Molecular-Level Dispersion of Graphene into Poly(vinyl alcohol) and Effective Reinforcement of their Nanocomposites. *Adv. Funct. Mater.* **19,** 2297-2302 (2009).